Liouville-space pathways for spectral diffusion in photon statistics from single molecules

František Šanda and Shaul Mukamel*
Department of Chemistry, University of California, Irvine, California 92697, USA
(Received 5 August 2004; published 11 March 2005)

The factorial moments of photon counting statistics from a single molecule coupled to a quantum bath are expressed in terms of multipoint quantum correlation functions and represented by double-sided Feynman diagrams, in close formal analogy with nonlinear spectroscopy. At infinite temperature we recover the results of stochastic models of spectral diffusion where the bath dynamics is independent on the state of the system and the moments are described by lower-order correlation functions.

DOI: 10.1103/PhysRevA.71.033807 PACS number(s): 42.50.Ar, 42.50.Lc

I. INTRODUCTION

Photon counting experiments have been carried out on ensembles of molecules since the seventies [1–4]. Recent advances in single molecule spectroscopy provide detailed information about enviroment fluctuations in the condensed phase which is not available from bulk measurements [5–12].

Statistical analysis of photon counting has been used to distinguish between static (inhomogenous) and fast (homogenous) fluctuations of molecular parameters (e.g., frequencies, donor-acceptor distances, and kinetic rates), through correlations between individual photon emission events. Statistical properties of photon counting are commonly described using either correlation functions or factorial moments. The Mandel parameter is a combination of moments widely used as a direct test for deviations from Poissonian statistics [4]. Photon counting statistics was originally formulated in terms of correlation functions of the electric field [4,13,14]. However, for single molecule experiments it is more natural to recast it in terms of molecular correlation functions.

One measure of a nonclassical state of the radiation field is photon antibunching. This effect which reflects the inability of a two level system to emit two photons in a short time interval has been described using the Bloch equations for a single two level atom [15–17]. More detailed single-molecule experiments carried out over the past two decades [5–8] focused on bath-induced spectral properties. The stochastic behavior of single molecule trajectories was widely studied [11,18–20].

A stochastic two state sudden jump model of spectral diffussion [21,22] was recently used to express the second factorial moment in the terms of four-time correlation functions [12,23]. A perturbative weak-field solution of the Bloch equations was used to investigate the influence of frequency fluctuations on the emitted light intensity. Microscopic simulations of photon counting experiments require the conditional probabilities for different photon count histories, and a resetting procedure [24] which specifies the state of the system after the emission event. Monte Carlo wave-function techniques were utilized to calculate both fluctuation and quantum-mechanical effects [25,26]. The generating function formalism [13,14,27] was employed to study spectral diffussion resulting from stochastic frequency fluctuations [28,29]. However, stochastic models [12,22,28–34] only apply in the infinite temperature limit, where the effect of the system on the bath is negligible and, consequently, they have some inherent limitations, e.g., they cannot account for the fluorescence Stokes shift [35], which is an important direct signature of spectral diffusion.

In this paper we develop a perturbation theory for the moments of photon counting statistics from a two level system driven by a classical optical field and coupled to a finite temperature quantum bath. In Sec. II we show how photon counting observables can be calculated using the generating function approach. The only approximation made is that spontaneous emission is described by a master equation [36]. The factorial moments for a two level model undergoing spectral diffusion are calculated in Sec. III. All observables are recast in terms of multipoint bath correlation functions which are expressed both in Liouville space and in Hilbert space. The second factorial moment of the photon count which determines the Mandel parameter is calculated. Application is made to a Brownian oscillator model of the bath. In Appendix A we present rules for constructing double-sided Feynman diagrams for factorial moments, which resemble those used in ultrafast nonlinear spectroscopy [35]; the fundamental connection between the two observables is thus established. The connection to stochastic models is finally disscused in Sec. IV.

II. GENERATING FUNCTIONS FOR SINGLE-PHOTON COUNTING OBSERVABLES

The most fundamental physical quantity which carries the complete information contained in single-photon counting measurements is the joint probability density $P^{(n)}(t_0;\tau_1,\tau_2,\ldots,\tau_n;t)$, to detect n photons during the observation window (between t_0 and t), the first photon emitted at time τ_1, the second at time τ_2, etc. Other less-detailed observables do not monitor individual photons, but record the number $n(t)$ of emitted photons in a given time window. $n(t)$ is connected to the time resolved fluorescence intensity:

*Email address: smukamel@uci.edu

$$I(t) \equiv \frac{n(t+\Delta t) - n(t)}{\Delta t}, \quad \Delta t \to 0. \tag{1}$$

We focus on two common steady-state observables. The autocorrelation function $h^{(2)}$ of fluorescence intensities I is defined by

$$h^{(2)}(\tau) \equiv \frac{\langle I(t+\tau)I(t)\rangle}{\langle I(t+\tau)\rangle\langle I(t)\rangle}. \tag{2}$$

Multipoint quantities can be defined in a similar way. It follows directly from these definitions that $h^{(2)}$ is related to $P^{(n)}$ by

$$h^{(2)}(\tau) = \frac{1}{\langle I\rangle^2}\Bigg(P^{(2)}(t_0;t_0,t_0+\tau;t_0+\tau) + \int_{t_0}^{t_0+\tau} d\tau_1 P^{(3)}(t_0;t_0,\tau_1,t_0+\tau;t_0+\tau) + \int_{t_0}^{t_0+\tau} d\tau_2 \int_{t_0}^{\tau_2} d\tau_1 P^{(4)}(t_0;t_0,\tau_1,\tau_2,t_0+\tau;t_0+\tau) + \cdots \Bigg). \tag{3}$$

At steady state $h^{(2)}$ is independent on the initial time t_0. $P^{(2)}(\tau_1,\tau_2;\tau_1,\tau_2)$ and $h^{(2)}(\tau_2-\tau_1)$ differ by whether the emission is controlled during the (τ_1,τ_2) time interval. $P^{(2)}$ implies that only two photons were emitted during the observation period whereas $h^{(2)}$ does not specify the total number of photons.

For a two level model with no fluctuations or when the bath fluctuations are fast, the multitime probabilities may be factorized into products of two-time quantities,

$$h^{(n)}(\tau_1,\tau_2,\ldots\tau_{n-1}) = \prod_{i=1}^{n-1} h^{(2)}(\tau_i - \tau_{i-1}).$$

No additional information is then carried by high-order correlation functions since the bath is at equilibrium at all times. This factorization does not hold when fluctuations are slow, or when more than two levels are involved where the state of the bath (or the system) after emission may depend on the photon emission history. Memory thus builds up, and can be probed by higher-order correlation functions.

The probability of detecting precisely n photons during the $(t_0;t)$ observation window is

$$Q(n;t_0,t) = \int_{t_0}^{t}\int_{\tau_1}^{t}\cdots\int_{\tau_{n-1}}^{t} P^{(n)}(t_0;\tau_1,\tau_2,\ldots\tau_n;t)d\tau_1\cdots d\tau_n. \tag{4}$$

For a Poissonian process the probability $P^{(n)}(t_0;\tau_1,\tau_2,\ldots,\tau_n;t)=\lambda^n\exp[\lambda(t_0-t)n]$ is independent on the times τ_i so that $Q(n;t_0,t)=[\lambda(t-t_0)]^n/(n!)\times\exp[\lambda(t_0-t)n]$.

The mth factorial moment of the distribution is defined by

$$\langle n(n-1)\cdots(n-m+1)\rangle = \sum_k k(k-1)\cdots(k-m+1)Q(k,t_0,t). \tag{5}$$

A commonly used combination of moments is the Mandel parameter,

$$M(\tau) \equiv \frac{\langle n(n-1)\rangle - \langle n\rangle^2}{\langle n\rangle}. \tag{6}$$

$M=0$ ($M<0$) implies Poissonian (subpoissonian) statistics. Equation (5) shows that the Mandel parameter (as any other factorial moment) may be derived from the joint density P, but carries less information.

At steady state the Mandel parameter and the fluorescence autocorrelation function are connected [17,33,34]:

$$M(t) = \frac{2\langle I\rangle}{t}\int_0^t dt_1\int_0^{t_1} dt_2[h^{(2)}(t_2)-1]. \tag{7}$$

We next show how all these quantities may be conveniently calculated using the generating function formalism [4,13,14,27,29,37]. We consider a multilevel system with states $|i\rangle;|j\rangle\cdots$ described by the density matrix $\hat\rho$. Photon counting measures localized emission events in time, and spontaneous emission is adequately described by the master equation which has been derived microscopically starting with the quantum Hamiltonian of the radiation field [36]:

$$2\left(\frac{d\hat\rho}{dt}\right)_M = \sum_{ijkl}\gamma_{ij,kl}(-\hat S_{ij}^\dagger\hat S_{kl}\hat\rho + 2\hat S_{kl}\hat\rho\hat S_{ij}^\dagger - \hat\rho\hat S_{ij}^\dagger\hat S_{kl}), \tag{8}$$

where $\hat S_{ij}^\dagger \equiv |i\rangle\langle j|$; $\hat S_{ij}\equiv|j\rangle\langle i|$ are raising (lowering) operators connected with radiative transition from level $|i\rangle$ to a lower level $|j\rangle$.

Equation (8) is written in Hilbert space, where $\hat\rho$ is a matrix. We next transform it to Liouville space and adopt tetradic notation. The elements of Liouville space are $|jk\rangle\rangle \equiv |j\rangle\langle k|$ and ρ becomes a *vector* (rather than a matrix) in this higher space. Using this notation we can recast the master equation in the form

$$\left(\frac{d\hat\rho}{dt}\right)_M = \hat{\mathcal{R}}\hat\rho - \hat\Gamma\hat\rho, \tag{9}$$

where $\hat{\mathcal{R}}$ and $\hat\Gamma$ denote the positive and negative contributions to Eq. (8),

$$\hat{\mathcal{R}} \equiv \sum_{ijkl}|ij\rangle\rangle\gamma_{lj,ki}\langle\langle kl|;$$

$$2\hat\Gamma \equiv \sum_{ij,km}|ij\rangle\rangle\gamma_{im,km}\langle\langle kj| + \sum_{ijlm}|ij\rangle\rangle\gamma_{lm,jm}\langle\langle il|. \tag{10}$$

The *resetting superoperator* $\hat{\mathcal{R}}$ describes the observation of a photon [24]. For spectrally resolved detection we should include in the resetting matrix only those rates related to the observed transitions within the detection bandwidth.

The time evolution of the multilevel system is described by the system Hamiltonian H_S together with the Hamiltonian $\hat{H}_{SB}$ which describes the bath and its interaction with the system. We take $\hat{H}_{SB}$ to be of the form

$$\hat{H}_{SB} = \sum_j |j\rangle \hat{H}_{Bj}(\mathbf{q}) \langle j|, \tag{11}$$

where $\mathbf{q}$ are the quantum bath degrees of freedom. Equation (11) represents a general model of spectral diffusion whereby the system energies are modulated by the bath. The full time evolution is given by the Liouville equation

$$\frac{d\hat{\rho}}{dt} = -i[\hat{H}_S, \hat{\rho}] - i[\hat{H}_{SB}, \hat{\rho}] + \left(\frac{d\hat{\rho}}{dt}\right)_M. \tag{12}$$

We shall adopt superoperator notation in the bath space and define left $\mathcal{S}^{(L)}$ and right $\mathcal{S}^{(R)}$ superoperators which act on the ket and the bra, respectively,

$$\mathcal{S}^{(L)}\hat{\rho} \equiv \mathcal{S}\hat{\rho};$$

$$\mathcal{S}^{(R)}\hat{\rho} \equiv \hat{\rho}\mathcal{S}. \tag{13}$$

We further switch to the interaction picture by using the unitary transformation

$$\mathcal{U}(t) = \exp(i\hat{H}_{SB}t). \tag{14}$$

This transformation does not affect the state of the system since $\hat{H}_{SB}$ is diagonal in the system space, but has a nontrivial action on the bath,

$$\mathcal{U}(t) = \sum_j |j\rangle \exp(i\hat{H}_{Bj}(\mathbf{q})t)\langle j|.$$

In the following, quantities without a hat (^) correspond to the interaction representation. The system Hamiltonian H_S is transformed as

$$H_S(t) = \mathcal{U}(t)\hat{H}_S\mathcal{U}^\dagger(t)$$

and similarly the master equation and other superoperators are transformed according to

$$\mathcal{R}(t) = \mathcal{U}^{(L)}(t)\mathcal{U}^{(R)\dagger}(t)\hat{\mathcal{R}}\mathcal{U}^{(L)\dagger}(t)\mathcal{U}^R(t),$$

$$\Gamma(t) = \mathcal{U}^{(L)}(t)\mathcal{U}^{(R)\dagger}(t)\hat{\Gamma}\mathcal{U}^{(L)\dagger}(t)\mathcal{U}^R(t). \tag{15}$$

The Liouville equation in the interaction representation finally reads

$$\frac{\partial}{\partial t}\rho = \mathcal{L}(t)\rho = \mathcal{L}_S(t)\rho + R(t)\rho - \Gamma(t)\rho; \tag{16}$$

$\mathcal{L}_S(t) = -i[H_S(t), \ldots]$ describes evolution of the optically driven multilevel system.

To define the conditional density matrices for photon statistics, we partition the Liouville superoperator as

$$\mathcal{L}(t) = \mathcal{L}'(t) + \mathcal{R}(t), \tag{17}$$

where

$$\mathcal{L}'(t) \equiv \mathcal{L}_S(t) - \Gamma(t).$$

We further define the time evolution operator for the conditional density matrix when no photon is observed [29],

$$G(t_f;t_i) \equiv \exp_+ \int_{t_i}^{t_f} dt' \mathcal{L}'(t'), \tag{18}$$

the action of the resetting matrix $\mathcal{R}\rho$ gives the conditional density matrix after photon emission. The n-point distribution of photons is then [13,14,37]

$$P^{(n)}(t_0;\tau_1,\tau_2,\ldots,t_n;t) \equiv \mathrm{Tr} G(t;\tau_n)\mathcal{R}(\tau_n)\cdots\mathcal{R}(\tau_2)G(\tau_2;\tau_1)\mathcal{R}(\tau_1)G(\tau_1;t_0)\rho(t_0). \tag{19}$$

The generating superoperator is constructed by multiplying conditional density matrices describing the observation of n photons before time τ by a prefactor s^n, and summing

$$\begin{aligned}\overline{\mathcal{G}}(t,t_0;s) &\equiv \sum_{n=0}^{\infty} s^n \int_{t_0}^{t}\cdots\int_{t_0}^{\tau_3}\int_{t_0}^{\tau_2} G(t;\tau_n)\mathcal{R}(\tau_n)\cdots\mathcal{R}(\tau_2) \\ &\quad\times G(\tau_2;\tau_1)\mathcal{R}(\tau_1)G(\tau_1;t_0)d\tau_1 d\tau_2\cdots d\tau_n \\ &= \exp_+\int_{t_0}^{t}[\mathcal{L}'(\tau') + s\mathcal{R}(\tau')]d\tau'.\end{aligned} \tag{20}$$

Note that for $s=1$ the generating superoperator simply coincides with the evolution superoperator. Equation (20) can be also recast in a differential form [37],

$$\frac{d\overline{\mathcal{G}}(t,t_0;s)}{dt} = [\mathcal{L}(t) - (1-s)\mathcal{R}(t)]\overline{\mathcal{G}}(t,t_0;s), \quad \overline{\mathcal{G}}(t=t_0;s) = 1. \tag{21}$$

The generating function is finally obtained by tracing $\overline{\mathcal{G}}$ over all system and bath variables:

$$\mathcal{G}(t,s) \equiv \mathrm{Tr}[\overline{\mathcal{G}}(t,t_0;s)\rho(t_0)]. \tag{22}$$

We consider an optically driven molecule in a steady state. We formally switch the electric field adiabatically starting at $t=-\infty$ where the system was at equilibrium in the ground state with the distribution ρ_{eq}. The steady state is reached at t_0, and the density matrix at the beginning of the photon counting period is

$$\rho(t_0) = \exp_+\int_{-\infty}^{t_0}\mathcal{L}(\tau')d\tau'\rho_{eq}. \tag{23}$$

The generating function is obtained by combining Eq. (23) with Eqs. (20) and (22).

In Eq. (22) we calculate separately $\rho(t_0)$ [Eq. (23)] and the subsequent evolution [Eq. (20)]. It is possible to combine the two and derive a single-step expression for the generating function. To that end we define a function κ,

$$\kappa(\tau',t_0;s) \equiv 1 \text{ for } -\infty < \tau' < t_0,$$

$$\kappa(\tau',t_0;s) \equiv s \text{ for } t_0 < \tau' < \infty. \tag{24}$$

This function is equal to s (1) for $\tau' > t_0$ ($\tau' < t_0$) when emitted photons are counted (not counted). Using Eqs. (20) and (22)–(24) the generating function assumes the form

$$\mathcal{G}(t,t_0;s) = \mathrm{Tr}\exp_+\left(\int_{-\infty}^{t} d\tau'[\mathcal{L}'(\tau') + \kappa(\tau',t_0;s)\mathcal{R}(\tau')]\right)\rho_{eq}. \tag{25}$$

For independent events, the probabilities $Q(n;t)$ are simple convolutions of the arrival time distribution $P^{(2)}$. In Laplace space their contributions to the generating function can be summed

$$\tilde{\mathcal{G}}(z,s) = \frac{1}{s + \tilde{P}^{-1}(z)}, \tag{26}$$

where z is the Laplace conjugate to time and $\tilde{\mathcal{G}}(z,s) = \int_{t_0}^{\infty}\mathcal{G}(t,t_0,s)e^{-z(t-t_0)}dt$ is the Laplace transform of $\mathcal{G}$, and similarly for P.

The expectation values and factorial moments may be obtained by differentiating the generating function with respect to s:

$$\frac{\partial^m}{\partial s^m}\mathcal{G}(t,t_0;s)\big|_{s=1} = \langle n(n-1)\cdots(n-m+1)\rangle. \tag{27}$$

Using Eq. (6) the Mandel parameter is given by

$$M(t-t_0) = \frac{(\partial^2/\partial s^2)\mathcal{G}(t,t_0;s)\big|_{s=1}}{(\partial/\partial s)\mathcal{G}(t,t_0;s)\big|_{s=1}} - \frac{\partial}{\partial s}\mathcal{G}(t,t_0;s)\big|_{s=1}. \tag{28}$$

Finally, the n-point autocorrelation function Eq. (2) is

$$h^{(n)}(\tau_{n-1},\ldots\tau_1) = \frac{\langle \mathrm{Tr}\,\mathcal{R}\bar{\mathcal{G}}(\tau_{n-1},\tau_{n-2};s=1)\cdots\mathcal{R}\bar{\mathcal{G}}(\tau_1,t_0;s=1)\mathcal{R}\rho(t_0)\rangle}{\langle \mathrm{Tr}\,\mathcal{R}\rho(t_0)\rangle^n}. \tag{29}$$

III. PROBING SPECTRAL DIFFUSSION BY THE SECOND FACTORIAL MOMENT

We consider a molecule with two electronic levels (a ground state $|g\rangle$ and an excited state $|e\rangle$ with energy ϵ) which interacts with a resonant classical laser field with frequency ω. In the rotating wave approximation the system Hamiltonian is

$$\hat{H}_S = |e\rangle\epsilon\langle e| + E(t)e^{-i\omega t}|e\rangle\mu\langle g| + E^*(t)e^{i\omega t}|g\rangle\mu^*\langle e|, \tag{30}$$

where the transition dipole moment μ is assumed to be independent on $\mathbf{q}$ [38] and $E(t)$ is the slowly varying field envelope. $\hat{H}_{SB}$ [Eq. (11)] is now given by

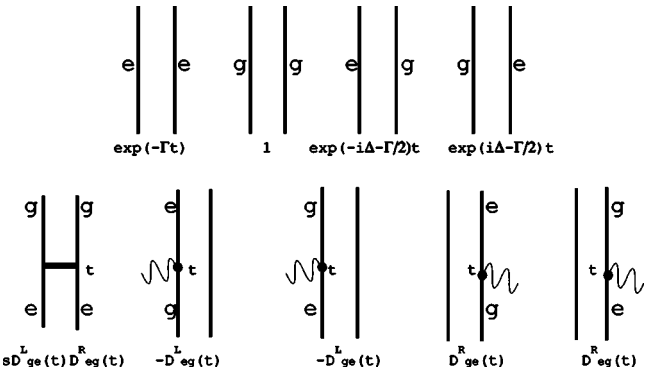

FIG. 1. Contributions to the generating function.

$$\hat{H}_{SB} = |g\rangle\hat{H}_g(\mathbf{q})\langle g| + |e\rangle\hat{H}_e(\mathbf{q})\langle e|. \tag{31}$$

The master equation [Eq. (9)] has the following tetradic matrix elements:

$$\hat{\mathcal{R}}_{gg,ee} = \Gamma, \quad \hat{\Gamma}_{ee,ee} = \Gamma, \quad \hat{\Gamma}_{eg,eg} = \Gamma/2, \quad \hat{\Gamma}_{ge,ge} = \Gamma/2. \tag{32}$$

All other elements of $\hat{\mathcal{R}}$ and $\hat{\Gamma}$ are zero.

In the interaction representation [Eq. (14)], the dipole moment operator is

$$D_{eg}(t) \equiv \mu\exp(i\hat{H}_e t)\exp(-i\hat{H}_g t),$$

$$D_{ge}(t) \equiv \mu^*\exp(i\hat{H}_g t)\exp(-i\hat{H}_e t), \tag{33}$$

and the master equation elements are obtained by combining Eq. (15) with Eq. (32),

$$\Gamma(t) = \hat{\Gamma},$$

$$\mathcal{R}(t) = (\hat{\mathcal{R}}_{gg,ee}/|\mu|^2)|gg\rangle\rangle D_{ge}^{(L)}(t)D_{eg}^{(R)}(t)\langle\langle ee|, \tag{34}$$

where the superoperator components $D_{eg}^{(L)}$ and $D_{eg}^{(R)}$ are defined by Eq. (13):

$$D_{eg}^{(L)}(t)\rho \equiv D_{eg}(t)\rho,$$

$$D_{eg}^{(R)}(t)\rho \equiv \rho D_{eg}(t), \tag{35}$$

and similarly for the conjugate operator $D_{ge}(t)$.

The generating function is obtained by solving Eqs. (20) and (22), or (25) perturbatively in the electric field. Details of the derivation for a general initial density matrix are given in Appendix B. The various contributions can be represented by double-sided Feynman diagrams [35] whose rules are given in Appendix A (See Fig. 1). The factorial moments are then obtained by differentiation with respect to s, Eq. (27).

We start with the canonical ground-state distribution $\rho_{eg} = \exp-\beta\hat{H}_g/\mathrm{Tr}_B\exp-\beta\hat{H}_g$ before the electric field is switched on. All Feynman diagrams start at $|gg\rangle\rangle$ at the bottom (Fig. 2). Equation (B9) can be recast in terms of the Liouville-space correlation functions:

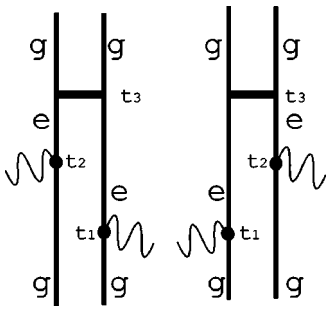

FIG. 2. Double sided Feynman diagrams for the first factorial moment at steady state to second (leading) order in the electric field.

$$\langle\langle \mathcal{S}_1^{\nu_1}(t_1)\cdots\mathcal{S}_n^{\nu_n}(t_n)\rangle\rangle_g \equiv \mathrm{Tr}_B \mathcal{S}_1^{\nu_1}(t_1)\cdots\mathcal{S}_n^{\nu_n}(t_n)\rho_{eg}; \quad (36)$$

where $\mathcal{S}_k^{\nu_k}$ are superoperators with $\nu=(L);(R)$, or in terms of Hilbert-space correlation function:

$$\langle \mathcal{S}_1(t_1)\cdots\mathcal{S}_n(t_n)\rangle_g \equiv \mathrm{Tr}_B \mathcal{S}_1(t_1)\cdots\mathcal{S}_n(t_n)\rho_{eg}, \quad (37)$$

where $\mathcal{S}_k$ are Hilbert-space operators.

We denote the time intervals $t_{ij}\equiv t_i - t_j$. The second-order contribution to the average photon count [Eq. (B12)] is represented by the two Feynman diagrams shown in Fig. 2. These diagrams come in complex conjugate pairs, e.g.,

$$\langle\langle D_{eg}^{(L)}(t_2)D_{ge}^{(R)}(t_1)\rangle\rangle_g^* = \langle\langle D_{ge}^{(R)}(t_2)D_{eg}^{(L)}(t_1)\rangle\rangle_g.$$

Introducing the two-time correlation function

$$J(t_2;t_1) \equiv \langle\langle D_{ge}^{(R)}(t_2)D_{eg}^{(L)}(t_1)\rangle\rangle_g = \langle D_{ge}(t_2)D_{eg}(t_1)\rangle_g,$$

the average photon count Eq. (B12) assumes the form

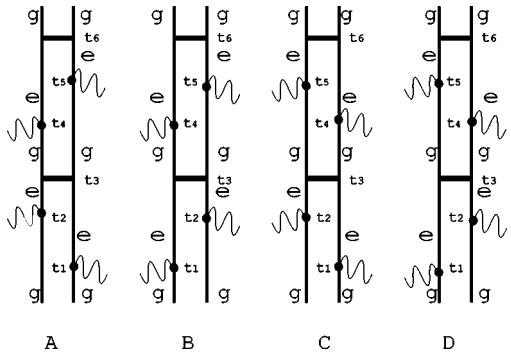

FIG. 3. Double sided Feynman diagrams for the second factorial moment at steady state to fourth (leading) order in the electric field.

$$\langle n\rangle(t;t_0) = \Gamma\int_{t_0}^{t}\int_{-\infty}^{t_3}\int_{-\infty}^{t_2} E^*(t_2)E(t_1) \times e^{-\Gamma t_{32}}e^{(i\Delta-\Gamma/2)t_{21}}J(t_2,t_1)dt_1dt_2dt_3 + \mathrm{c.c.}, \quad (38)$$

where $\Delta\equiv\omega-\epsilon$ is the laser detuning from the two level frequency ϵ. For a steady state created by continuous pumping with monochromatic light we simply set $E(t)=E$. Denoting $\tau=t_1-t_2$, and using time translation invariance of J, Eq. (38) then shows that the fluorescence intensity is proportional to the absorption line shape,

$$\langle n\rangle(t;t_0) = (t-t_0)E^2\int_{-\infty}^{0} e^{-(i\Delta-\Gamma/2)\tau}J(0,\tau)d\tau + \mathrm{c.c.} \quad (39)$$

The second factorial moment obtained by double differentiation of the generating function Eq. (B8) with respect to s [Eq. (27)] has a leading fourth order term in the electric field Eq. (B13):

$$\langle n(n-1)\rangle(t;t_0) = 2\frac{\Gamma^2}{|\mu|^2}\int_{t_0}^{t}dt_6\int_{t_0}^{t_6}dt_5\int_{t_0}^{t_5}dt_4\int_{t_0}^{t_4}dt_3\int_{-\infty}^{t_3}dt_2\int_{-\infty}^{t_2}dt_1 E^*(t_2)E(t_1)e^{-\Gamma(t_{65}+t_{32})} \times [E^*(t_5)E(t_4)e^{(i\Delta-\Gamma/2)t_{54}}e^{(i\Delta-\Gamma/2)t_{21}}\langle\langle D_{ge}^{(R)}(t_5)D_{eg}^{(L)}(t_4)D_{ge}^{(L)}(t_3)D_{eg}^{(R)}(t_3)D_{ge}^{(R)}(t_2)D_{eg}^{(L)}(t_1)\rangle\rangle_g + E(t_5)E^*(t_4)e^{(-i\Delta-\Gamma/2)t_{54}}e^{(i\Delta-\Gamma/2)t_{21}}\langle\langle D_{eg}^{(L)}(t_5)D_{ge}^{(R)}(t_4)D_{ge}^{(L)}(t_3)D_{eg}^{(R)}(t_3)D_{ge}^{(R)}(t_2)D_{eg}^{(L)}(t_1)\rangle\rangle_g] + \mathrm{c.c.} \quad (40)$$

The correlation functions do not depend on t_6 and this variable may be integrated out using $\int_{t_0}^{t}dt_6\int_{t_0}^{t_6}dt_5=\int_{t_0}^{t}dt_5\int_{t_5}^{t}dt_6$. Again, at steady state we simply set $E(t)=E$.

The regions of integration in Eq. [(40)] can be described as follows: the driving field is switched on prior to t_0 but the counting only starts at t_0 (this is why the t_3 integration which is connected with emission vertex starts at t_0). The t_4, t_5 integrations also start at t_0 since $t_4, t_5 > t_3$.

The second factorial moment [Eq. (40)] can be represented by the four Feynman diagrams given in Fig. 3. These diagrams are best understood using Eq. (7). We expect to be able to calculate the n time correlation function perturbatively, with the leading $2n$th order in the electric field. It is less obvious why we can describe the absorption and emission of a large number of photons n to low order in the field. At steady state the nth factorial moment is connected with an n time correlation function, and the factorial moments are obtained from correlation functions by integrations over possible n-tuples of observation times. For the first moment, we calculate the average photon count using Eq. (39). For the second factorial moment, the two emission lines in Fig. 3 represent the times when the detector is open to observe a photon. Our compact notation does not distinguish the two detection lines from the others, but the integer factor for each

graph (given by differentiation with respect to s) accounts for all possible choices of pairs of lines.

Let us consider the Feynman diagram for the second factorial moment given in Fig. 3(A). The molecule initially at equilibrium in the ground state interacts with the electric field, first with the bra (from the right) at time t_1, then with the ket (left) at time t_2. The propagation in $|ge\rangle\rangle$ between t_1 and t_2 includes the decay rate $\Gamma/2$ representing excited-state lifetime; pure dephasing is included in the bath correlation function. The excited-state evolution depends on the molecule-bath correlation. In our model, the spontaneous emission rate does not depend on the bath variables, and the average photon counting rate [Eq. (39)] can be calculated in the weak-field limit, independent on the subsequent relaxation. During t_{32} the molecule evolves in the excited state. At t_3 we observe the emitted photon and the molecule moves to the ground state. The excitation at times t_4 and t_5 and the second emission at time t_6 can be interpreted similarly. Depending on the spontaneous emission rate, the relaxation rate, and laser detuning, the molecule after the emission at t_3 may be in the nonstationary state. Thus the probability of subsequent absorption from the initial state may be different. Various emission events may become correlated, resulting in deviations from Poissonian distribution.

Equation (40) can be recast in the form

$$\langle n(n-1)\rangle(t,t_0) = 2E^4(\Gamma/|\mu|)^2 \int_{t_0}^{t} dt_6 \int_{t_0}^{t_6} dt_5 \int_{t_0}^{t_5} dt_4 \int_{t_0}^{t_4} dt_3 \int_{-\infty}^{t_3} dt_2 \int_{-\infty}^{t_2} dt_1 e^{-\Gamma(t_{65}+t_{32})} \times e^{-\Gamma(t_{54}+t_{21})/2}[e^{i\Delta(t_{54}+t_{21})}F(t_2,t_3,t_5,t_4,t_3,t_1) + e^{i\Delta(t_{45}+t_{21})}F(t_2,t_3,t_4,t_5,t_3,t_1)] + \text{c.c.} \tag{41}$$

with the six point Hilbert-space correlation function

$$F(t_1,t_2,t_3,t_4,t_5,t_6) \equiv \langle D_{ge}(t_1)D_{eg}(t_2)D_{ge}(t_3)D_{eg}(t_4)D_{ge}(t_5)D_{eg}(t_6)\rangle_g.$$

The Hilbert-space expression is less transparent compared to its Liouville-space counterpart [Eq. (40)] since it mixes time variables coming from the evolution of the bra and the ket. The quantum treatment of the bath allows us to present the factorial moments using Hilbert-space correlation functions. Stochastic approaches which are not based on a Hamiltonian for the bath can only be represented by Liouville-space correlation functions.

Closed expressions for the correlation functions can be derived for the Brownian oscillator (spin boson) model for the bath [35,39],

$$\hat{H}_g = \sum_j \left(\frac{p_j^2}{2m_j} + \frac{1}{2} m_j \omega_j^2 q_j^2 \right),$$

$$\hat{H}_e = \sum_j \left(\frac{p_j^2}{2m_j} + \frac{1}{2} m_j \omega_j^2 (q_j + d_j)^2 - \frac{1}{2} m_j \omega_j^2 d_j^2 \right). \tag{42}$$

We define the energy gap between the ground- and excited-state Hamiltonians $\hat{U}(\mathbf{q}) \equiv \hat{H}_e - \hat{H}_g$. Its time evolution with respect to the ground-state Hamiltonian is

$$U(\tau) \equiv \exp(i\hat{H}_g\tau)\hat{U}\exp(-i\hat{H}_g\tau). \tag{43}$$

We further introduce the auxiliary line broadening function:

$$g(t) \equiv \int_0^t \int_0^{\tau_1} \langle U(\tau_1)U(\tau_2)\rangle d\tau_1 d\tau_2 \equiv g'(t) + ig''(t). \tag{44}$$

The correlation functions for this model are calculated in Appendix E using the second-order cumulant expansion. We then have

$$J(t_1,t_2) = |\mu|^2 \exp[-g(t_{12})]$$

$$F(t_1,t_2,t_3,t_4,t_2,t_6) = |\mu|^6 \exp[g(t_{13}) - g(t_{14}) - g(t_{16}) - g(t_{34}) - g(t_{36}) + g(t_{46}) - 2ig''(t_{23}) + 2ig''(t_{24})]. \tag{45}$$

$g(t)$ may be recast in terms of the bath spectral density $C''(\omega)$ (The Fourier transform of the imaginary part of $\langle U(t)U(0)\rangle$):

$$g(t) = \frac{1}{2\pi}\int_{-\infty}^{\infty} d\omega \frac{1-\cos(\omega t)}{\omega^2} \coth(\beta\omega/2)\tilde{C}''(\omega) - \frac{i}{2\pi}\int_{-\infty}^{\infty} d\omega \frac{\sin(\omega t) - \omega t}{\omega^2}\tilde{C}''(\omega).$$

For the overdamped Brownian oscillator spectral density

$$\tilde{C}''(\omega) = 2\lambda \frac{\omega\Lambda}{\omega^2 + \Lambda^2},$$

where $\lambda = \Sigma_j (1/2\hbar) m_j \omega_j^2 d_j^2$ is the coupling strength to the bath and Λ represents its relaxation rate, in the high- (but not infinite) temperature limit $\beta\Lambda \ll 1$ we obtain

$$g(t>0) = \frac{2\lambda}{\beta\Lambda^2}[\exp(-\Lambda t) + \Lambda t - 1] - i(\lambda/\Lambda)[\exp(-\Lambda t) + \Lambda t - 1],$$

$$g(-t) = g^*(t). \tag{46}$$

The correlation functions are finally obtained by substituting Eq. (46) in Eq. (45). The sixth point correlation function for the relevant time ordering $t_4, t_3 > t_2 > t_1 > t_6$ is

$$\begin{aligned} F(t_1,t_2,t_3,t_4,t_2,t_6) = |\mu|^6 \exp\Bigg(& \frac{2\lambda}{\beta\Lambda^2}(e^{-\Lambda t_{31}} - e^{-\Lambda t_{41}} - e^{-\Lambda t_{16}} \\ & - e^{-\Lambda|t_{34}|} - e^{-\Lambda t_{36}} + e^{-\Lambda t_{46}} + 2) \\ & - \frac{i\lambda}{\Lambda}(- e^{-\Lambda t_{31}} + e^{-\Lambda t_{41}} - e^{-\Lambda t_{16}} \pm e^{-\Lambda|t_{34}|} \\ & - e^{-\Lambda t_{36}} + e^{-\Lambda t_{46}} + 2e^{-\Lambda t_{32}} - 2e^{-\lambda t_{42}} + 2) \\ & - \frac{2\lambda}{\beta\Lambda}(|t_{34}| + t_{16}) + i\lambda(t_{16} + t_{34})\Bigg). \end{aligned} \tag{47}$$

The upper (lower) sign corresponds to $t_4 > t_3$ ($t_3 > t_4$) ordering. The second factorial moment is finally obtained by substituting Eq. (47) in Eq. (41).

Some care should be taken to calculate the steady state, the averaged photon count, and the second factorial moment at the same level of approximation. For the Mandel parameter, the leading quadratic term (in time) for the second factorial moment and squared intensity should exactly cancel. Any difference introduced by approximations can cause a large error for long binning times, therefore one must use consistent approximations. For the autocorrelation function this means that we need to reproduce $h^{(2)}=1$ for long times.

The correct asymptotic behavior for long binning times (compared to the radiative lifetime) $T=t-t_0\to\infty$ can be obtained by factorizing the bath correlation function,

$$\begin{aligned} &(1/|\mu|)^2\langle D_{ge}(t_2)D_{eg}(t_3)D_{ge}(t_5)D_{eg}(t_4)D_{ge}(t_3)D_{eg}(t_1)\rangle_g \\ &\quad = \langle D_{ge}(t_2)D_{eg}(t_1)\rangle_g \langle D_{ge}(t_5)D_{eg}(t_4)\rangle_g. \end{aligned}$$

This holds for long delays between photon absorption events $|t_4-t_3| \gg |t_2-t_1|; |t_5-t_4|, \Lambda^{-1}$. By integrating Eq. (40) over t_3, t_6, we get for long binning times $T\to\infty$ that the dominating quadratic coefficient of the second factorial moment is equal to the squared cofficient for the linear term of the average photon count,

$$\begin{aligned} &\frac{2}{T^2}\int_0^T dt_4 \int_0^{t_4} dt_3 \int_0^{t_3} dt_2 \int_0^{t_2} dt_1 e^{(i\Delta-\Gamma/2)(t_{43}+t_{21})} \langle D_{ge}(t_4)D_{eg}(t_3)\rangle \\ &\quad \times \langle D_{ge}(t_2)D_{eg}(t_1)\rangle \\ &\quad \simeq \left(\frac{1}{T}\int_0^T dt_2 \int_0^{t_2} dt_1 e^{(i\Delta-\Gamma/2)(t_{21})} \langle D_{ge}(t_2)D_{eg}(t_1)\rangle\right)^2, \end{aligned} \tag{48}$$

Generally, the Mandel parameter approaches a constant limiting value for ergodic systems and large binning times. This is satisfied by Eq. (48).

The correlation function may be calculated from the second factorial moment by rewriting Eq. (7) as

$$h^{(2)}(t-t_0) = \frac{(t-t_0)^2}{2\langle n(t,t_0)\rangle^2} \frac{d^2\langle n(n-1)\rangle}{dt^2}. \tag{49}$$

Using Eq. (B13) and

$$\frac{d^2}{dt^2}\int_{t_0}^t \int_{t_0}^{t_2} e^{-\Gamma(t_2-t_1)} G(t_1) dt_2 dt_1 = G(t) - \Gamma \int_{t_0}^t e^{-\Gamma(t-t_1)} G(t_1) dt_1$$

we get

$$\begin{aligned} h^{(2)}(t-t_0) = & \frac{E^4(t-t_0)^2\Gamma^2}{\langle n\rangle^2|\mu|^2} \int_{t_0}^t dt_4 \int_{t_0}^{t_4} dt_3 \int_{-\infty}^{t_3} dt_2 \int_{-\infty}^{t_2} dt_1 e^{-\Gamma t_{32}} e^{(i\Delta-\Gamma/2)t_{21}} \\ & \times [e^{(i\Delta-\Gamma/2)(t-t_4)} \langle\langle D_{ge}^{(R)}(t) D_{eg}^{(L)}(t_4) D_{ge}^{(L)}(t_3) D_{eg}^{(R)}(t_3) D_{ge}^{(R)}(t_2) D_{eg}^{(L)}(t_1)\rangle\rangle_g \\ & + e^{(-i\Delta-\Gamma/2)(t-t_4)} \langle\langle D_{eg}^{(L)}(t) D_{ge}^{(R)}(t_4) D_{ge}^{(L)}(t_3) D_{eg}^{(R)}(t_3) D_{ge}^{(R)}(t_2) D_{eg}^{(L)}(t_1)\rangle\rangle_g] \\ & - \frac{E^4(t-t_0)^2\Gamma^3}{\langle n\rangle^2|\mu|^2} \int_{t_0}^t dt_5 \int_{t_0}^{t_5} dt_4 \int_{t_0}^{t_4} dt_3 \int_{-\infty}^{t_3} dt_2 \int_{-\infty}^{t_2} dt_1 e^{-\Gamma(t-t_5)} e^{-\Gamma t_{32}} e^{(i\Delta-\Gamma/2)t_{21}} \\ & \times [e^{(i\Delta-\Gamma/2)(t_5-t_4)} \langle\langle D_{ge}^{(R)}(t_5) D_{eg}^{(L)}(t_4) D_{ge}^{(L)}(t_3) D_{eg}^{(R)}(t_3) D_{ge}^{(R)}(t_2) D_{eg}^{(L)}(t_1)\rangle\rangle_g \\ & + e^{(-i\Delta-\Gamma/2)(t_5-t_4)} \langle\langle D_{eg}^{(L)}(t_5) D_{ge}^{(R)}(t_4) D_{ge}^{(L)}(t_3) D_{eg}^{(R)}(t_3) D_{ge}^{(R)}(t_2) D_{eg}^{(L)}(t_1)\rangle\rangle_g] + \text{c . c.} \end{aligned} \tag{50}$$

In Hilbert space Eq. (50) reads

$$\begin{aligned} h^{(2)}(t-t_0) = & \frac{E^4(t-t_0)^2\Gamma^2}{\langle n\rangle^2|\mu|^2} \int_{t_0}^t dt_4 \int_{t_0}^{t_4} dt_3 \int_{-\infty}^{t_3} dt_2 \int_{-\infty}^{t_2} dt_1 e^{-\Gamma t_{32}} e^{(i\Delta-\Gamma/2)t_{21}} \times [e^{(i\Delta-\Gamma/2)(t-t_4)} F(t_2,t_3,t,t_4,t_3,t_1) \\ & + e^{(-i\Delta-\Gamma/2)(t-t_4)} F(t_2,t_3,t_4,t,t_3t_1)] - \frac{E^4(t-t_0)^2\Gamma^3}{\langle n\rangle^2|\mu|^2} \int_{t_0}^t dt_5 \int_{t_0}^{t_5} dt_4 \int_{t_0}^{t_4} dt_3 \int_{-\infty}^{t_3} dt_2 \int_{-\infty}^{t_2} dt_1 e^{-\Gamma(t-t_5)} e^{-\Gamma t_{32}} e^{(i\Delta-\Gamma/2)t_{21}} \\ & \times [e^{(i\Delta-\Gamma/2)t_{54}} F(t_2,t_3,t_5,t_4,t_3,t_1) + e^{(-i\Delta-\Gamma/2)t_{54}} F(t_2,t_3,t_4,t_5,t_3,t_1)] + \text{c . c.} \end{aligned} \tag{51}$$

Higher factorial moments can be calculated in a similar way. The third factorial moment to sixth order in the electric field is given in Appendix D.

IV. COMPARISON WITH STOCHASTIC MODELS

Photon counting is usually calculated using stochastic models [28–31] described by the stochastic Liouville equation [22] which assumes that the bath evolution is independent on the state of the system. Common models of the bath are the multistate jump or the collective Gaussian coordinate. To compare our microscopic expressions with stochastic models we note that for classical stochastic models, the left (ket) and right (bra) bath density-matrix variables are identical, which gives

$$(1/|\mu|^2)D_{ge}^{(L)}(t)D_{eg}^{(R)}(t) \to (1/|\mu|^2)D_{eg}^{\dagger}(t)D_{eg}(t) = 1. \quad (52)$$

In this relation, the dipole moments are considered as stochastic c-number variables $[D_{ge}(t)=D_{eg}^{*}(t)]$ rather than operators in the bath Hilbert space. Applying Eq. (52) to the contributions to the factorial moment given in Appendix A, the time variable associated with the emission event can be integrated out giving

$$\int_{t_0}^{t_{k+1}} dt_k e^{-\Gamma(t_k-t_{k-1})}(\Gamma/|\mu|^2)D_{ge}^{(L)}(t_k)D_{eg}^{(R)}(t_k)\cdots \to [\xi(t_{k-1}) - e^{-\Gamma(t_{k+1}-t_{k-1})}]\cdots, \quad (53)$$

where $\xi(t)=1$ for $t>t_0$ and $\exp-\Gamma(t_0-t)$ for $t_0>t$. For stochastic models the six point correlation function thus reduces to a four point function,

$$K(t_1,t_2,t_3,t_4) = \langle D_{ge}(t_4)D_{eg}(t_3)D_{ge}(t_2)D_{eg}(t_1)\rangle = \langle D_{eg}^{*}(t_4)D_{eg}(t_3)D_{eg}^{*}(t_2)D_{eg}(t_1)\rangle.$$

Substituting Eq. (53) in Eq. (40) gives

$$\langle n(n-1)\rangle(t;t_0) = 2E^4(\Gamma/|\mu|)^2\int_{t_0}^{t}dt_4\int_{t_0}^{t_4}dt_3\int_{-\infty}^{t_3}dt_2\int_{-\infty}^{t_2}dt_1 \times(\xi(t_2)-e^{-\Gamma(t_3-t_2)})(1-e^{-\Gamma(t-t_4)}) \times e^{(i\Delta-\Gamma/2)t_{21}}[e^{(i\Delta-\Gamma/2)t_{43}}K(t_1,t_2,t_3,t_4) + e^{(-i\Delta-\Gamma/2)t_{43}}K(t_1,t_2,t_4,t_3)] + \text{c . c.} \quad (54)$$

This result can be obtained for the Brownian oscillator bath Eq. (45) by neglecting the imaginary part of g. The correlation function Eq. (45) then becomes independent on the emission time (t_2).

The reduction to a four point quantity and the transformation (53) are a direct consequence of the stochastic model for the bath: The bath does not respond to the system, its evolution does not depend on whether the system is in the ground state or in the excited state, and consequently the diagram does not depend on the emission time t_3.

The effect of Eq. (53) can be also seen by including the matrix $\mathcal{W}$ [Eq. (B3)] that describes the emission into the free Liouville operator $\mathcal{L}_0$ Eq. (B2). Direct exponentiation [for $(t>t_0)$]

$$\exp(A+\mathcal{W})t = \begin{pmatrix} \exp-\Gamma t & 0 \\ s(1-\exp-\Gamma t) & 1 \end{pmatrix} \quad (55)$$

gives the free Green function, which now has also off diagonal gg,ee elements. The corresponding Feynman diagrams can be described as follows: Assume that the system starts at t_1 in the excited state $|ee\rangle\rangle$, emits a photon at t_2, and then propagates in the ground state $|gg\rangle\rangle$ to t_3. For this process we assign the factor $s[1-\exp-\Gamma(t_1-t_3)]$ independent on the time t_2 in the emission vertex. Stated differently, we have a two time factor (Green function) not only for $ee\to ee$; $eg\to eg; ge\to ge; gg\to gg$, but also for propagation with emission $ee\to gg$ somewhere between these times.

In the Schrödinger picture, the stochastic model can be introduced in the following way: consider the Green function $\mathcal{G}$ describing $\hat{H}_g$ propagation on the ground state and $\hat{H}_e$ on the excited level. The perturbation theory is represented by the same Feynman diagrams (Fig. 3), the dipole moments are constant while the Green function represents a nontrivial evolution in the bath Liouville space. For instance, the Feynman diagram in Fig. 3(A) represents $\langle \mathcal{G}_{ge,ge}(t_{54})\mathcal{G}_{gg,gg}(t_{43})\mathcal{G}_{ee,ee}(t_{32})\mathcal{G}_{eg,eg}(t_{21})\rangle$. For stochastic models models the bath evolution is independent on the state of system so that $\mathcal{G}_{gg,gg}=\mathcal{G}_{ee,ee}$. We can therefore combine the two Green functions and obtain

$$\langle \mathcal{G}_{ge,ge}(t_{54})\mathcal{G}_{gg,gg}(t_{43})\mathcal{G}_{ee,ee}(t_{32})\mathcal{G}_{eg,eg}(t_{21})\rangle = \langle \mathcal{G}_{ge,ge}(t_{54})\mathcal{G}_{ee,ee}(t_{42})\mathcal{G}_{eg,eg}(t_{21})\rangle. \quad (56)$$

The t_{42} evolution is either in the ground state or in the excited state and the correlation function does not depend on t_3. To complete the contribution of a particular Feynman diagram one must multiply by the decay factors $e^{-\Gamma t_{21}/2}, e^{-\Gamma t_{54}/2}$, and $e^{-\Gamma t_{32}}$ respectively. The independence on the emission time is a fundamental difference between stochastic and microscopic models.

In the slow fluctuation regime (compared with the radiative rate), the bath hardly changes during the excited-state evolution, and the use of stochastic models is well justified. The Stokes shift is most relevant in the intermediate regime when the bath and spontaneous emission rates are comparable. The collective coordinate is very different for the microscopic and stochastic models, as its center elvolves in a different way in the excited state. Also antibunching on the Γ^{-1} time scale is not dominant in this regime, unlike the fast relaxation regime. The effect of detuning is expected to be significant. For resonant excitation (Fig. 4) the coordinate moves on the excited state towards the center of excited level and after emission, there will be a short delay for relaxation near the ground-state minimum, where the absorption occurs. This contributes to antibunching. In contrast, the stochastic model coordinate is still near the center of the ground state. For small detunings (Fig. 5) the excited-state wave packet moves in opposite directions in the stochastic and in the microscopic models. The microscopic model wave packet relaxes through the region of high absorbance causing significant photon bunching which is absent in the stochastic model.

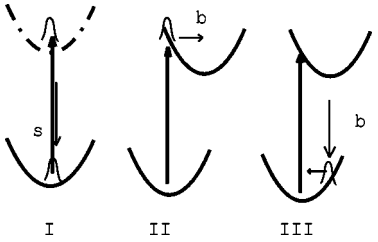

FIG. 4. The Stokes shift for resonant excitation. I: Stochastic wave packet is centered at the origin: its mean does not change with time. II: The Brownian oscillator model: the center of the wave packet during the excited state propagation moves towards the excited state origin. III: Following photon emission, the wave packet relaxes back to the ground state origin.

Recent studies had used a semiclassical definition of photon counting [12,23]. This approach introduces the stochastic photon count variable $n(x)$ for a given realization x of stochastic bath variable. n is calculated to second order in the electric field. The average photon count $\langle n(x)\rangle$ and higher moments $\langle n^2(x)\rangle$, etc., are then defined as the average over realizations of x. Formally, the semiclassical approximation differs from the exact microscopic formulation Eq. (40) in several ways. (i) Since the bath is treated classically, the second factorial moment is given by a four point rather than a six point correlation function. (ii) The semiclassical expressions contain additional nonphysical non-time-ordered terms which never show up in the exact formulation. (iii) Photon antibunching is not accounted for by the semiclassical approach.

In conclusion, we have developed a microscopic correlation-function theory of photon counting statistics by employing a generating function approach to describe statistical quantities connected with single molecule spectroscopy. A perturbative expansion in the electric field was carried out for an optically driven two level model and stochastic models were generalized to include a quantum model of the bath. This allows us to identify possible signatures of the time-dependent Stokes shift in photon statistics. The factorial moments and the autocorrelation functions were calculated for steady-state excitation and represented by double sided Feynman diagrams. The factorial moments may be expressed in terms of either Liouville-space or Hilbert-space bath correlation functions. Stochastic models involve a loss of information: the second factorial moment is independent on the emission time thereby reducing the six point to a four point correlation function. The differences between the microscopic and stochastic model should be most pronounced for fluctuations on the order of radiative decay time scale.

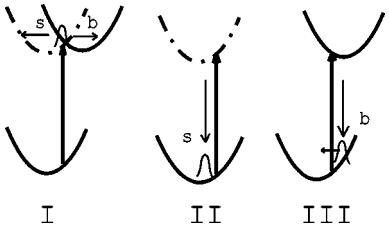

FIG. 5. The Stokes shift for small detuning. I: After excitation the wave packet evolves in opposite directions for (s) stochastic (dash potential) and (b) Brownian oscillator bath model (solid potential). II: Following emission, the stochastic wave packet is near equilibrium. III: Following emission, the Brownian oscillator wave packet relaxes through the region of high absorbance, causing photon bunching.

ACKNOWLEDGMENTS

The support of the National Science Foundation (Grant No. CHE-0132571) and NIRT (Grant No. EEC 0303389) and the Air Force Office of Scientific Research (Grant No. FA9550–04–10332) is gratefully acknowledged.

APPENDIX A: FEYNMAN DIAGRAMS FOR THE FACTORIAL MOMENTS

Specific contributions to the factorial moments can be represented graphically. Below we give the rules for constructing the double sided Feynman diagrams representing Eqs. (B7) and (B8).

(i) Two vertical lines represent the density matrix, time runs from bottom to top. Each line has for a given time either the value e (excited state) or g (ground state).

(ii) Vertical lines running through the time interval τ are assigned the following factors: (a) gg line: factor 1; (b) ge line: factor $e^{-(i\Delta+\Gamma/2)\tau}$; (c) eg line: factor $e^{(i\Delta-\Gamma/2)\tau}$; (d) ee line: factor $\exp(-\Gamma\tau)$.

(iii) Photon emission is represented by a bold horizontal line changing the state $ee\rightarrow gg$ on the vertical lines. It carries a factor $(s\Gamma/|\mu|^2)D_{ge}^{(L)}(t)D_{eg}^{(R)}(t)$, for calculation of the generating function using Eq. (20) or $[\kappa(t,t_0;s)\Gamma/|\mu|^2]D_{ge}^{(L)}(t)D_{eg}^{(R)}(t)$ when the generating function for the stationary state is calculated using Eq. (25).

(iv) Wavy lines represent interactions with the optical field, changing the particular line $e\rightarrow g$ or $g\rightarrow e$. Each interaction has a factor i; altogether the diagram has factor $(i)^K$, where K is the order, i.e., number of wavy lines in graph. Factors $\pm D_{eg;ge}^{(L;R)}(t)$ are assigned by the following rules (see Fig. 1):

(a) left side: $g\rightarrow e$, $-E(t)D_{eg}^{(L)}(t)$, $e\rightarrow g$, $-E^*(t)D_{ge}^{(L)}(t)$;

(b) right side: $g\rightarrow e$, $E^*(t)D_{ge}^{(R)}(t)$, $e\rightarrow g$, $E(t)D_{eg}^{(R)}(t)$.

After assigning the correct factor to each diagram, summation finally gives the generating function. For calculating the nth factorial moment all diagrams with n or more emission lines should be included. (Note that k emission implies that there are least $2k$ interactions in the diagram. Therefore the number of diagrams for a given order in the electric field is finite.) Their factors are summed up and nth derivative in s should be taken to obtain the nth factorial moment. To avoid s derivatives of Eq. (20) an additional factor $m(m-1)\cdots(m-n+1)$ is assigned, where m is the number of horizontal thick emission lines.

APPENDIX B: THE GENERATING FUNCTION

In this appendix we derive the generating function Eq. (22) and the factorial moments for the model introduced in

Eqs. (30)–(32). In Liouville space, the electron-density matrix is a four-dimensional vector:

$$\rho = (\rho_{ee}(\mathbf{q};\mathbf{q}'),\ \rho_{gg}(\mathbf{q};\mathbf{q}'),\ \rho_{eg}(\mathbf{q};\mathbf{q}')e^{i\omega t},\ \rho_{ge}(\mathbf{q};\mathbf{q}')e^{-i\omega t}),$$

where $\mathbf{q}$ is the ket bath variable and $\mathbf{q}'$ is the bra variable of density matrix. We further represent the electric field [Eq. (30)] $E(t)=Ef(t)$; where the intensity of the field E serves as a formal parameter of perturbative expansion and $f(t)$ is the slowly varying function, which is set to 1 for continuous-wave experiment.

We partition the Liouville operator Eq. (16) into a free part and perturbation:

$$\mathcal{L} + (\kappa - 1)R = \mathcal{L}_0 + \mathcal{L}_{int}, \quad \mathcal{L}_0 = \begin{pmatrix} A & 0 \\ 0 & B \end{pmatrix},$$

$$\mathcal{L}_{int}(t,s) = \begin{pmatrix} \mathcal{W}(t,s) & \mathcal{V}(t) \\ \mathcal{V}(t) & 0 \end{pmatrix} \tag{B1}$$

with the 2×2 blocks

$$A = \begin{pmatrix} -\Gamma & 0 \\ 0 & 0 \end{pmatrix}, \quad B = \begin{pmatrix} i\Delta - \Gamma/2 & 0 \\ 0 & -i\Delta - \Gamma/2 \end{pmatrix}; \tag{B2}$$

$$\mathcal{V} = iE\begin{pmatrix} f^*(t)D_{ge}^{(R)}(t) & -f(t)D_{eg}^{(L)}(t) \\ -f^*(t)D_{ge}^{(L)}(t) & f(t)D_{eg}^{(R)}(t) \end{pmatrix},$$

$$\mathcal{W} = \frac{\kappa(t,t_0;s)\Gamma}{|\mu|^2}\begin{pmatrix} 0 & 0 \\ D_{ge}^{(L)}(t)D_{eg}^{(R)}(t) & 0 \end{pmatrix}; \tag{B3}$$

and $\Delta \equiv \omega - \epsilon$ is the laser detuning from the two level frequency ϵ.

The free part [Eq. (B2)] of the Liouville operator can be directly exponentiated:

$$\exp At = \begin{pmatrix} \exp -\Gamma t & 0 \\ 0 & 1 \end{pmatrix},$$

$$\exp Bt = \begin{pmatrix} \exp -(\Gamma/2 - i\Delta)t & 0 \\ 0 & \exp -(\Gamma/2 + i\Delta)t \end{pmatrix}. \tag{B4}$$

We expand the generating superoperator [Eq. (25)] perturbatively in $\mathcal{L}_{int}$ with the transformation:

$$\tilde{\bar{\mathcal{G}}}(t,t_0;s) = \exp(-\mathcal{L}_0 t)\bar{\mathcal{G}}(t,t_0;s),$$

$$\tilde{\mathcal{L}}_{int}(t,s) = \exp -\mathcal{L}_0 t \mathcal{L}_{int} \exp \mathcal{L}_0 t = \begin{pmatrix} \exp -At\mathcal{W}(t)\exp At & \exp -At\mathcal{V}(t)\exp Bt \\ \exp -Bt\mathcal{V}(t)\exp At & 0 \end{pmatrix}. \tag{B5}$$

Our goal is to expand the photon statistics observables perturbatively in the electric field. Note that even though the emission matrix $\mathcal{W}(t,s)$ is formally included perturbatively, the matrix $\mathcal{W}$ is nilpotent (i.e., $\mathcal{W}^2=0$) and the generating function is given by a finite sum for a given order in electric field. $\mathcal{W}$ is thus included exactly and the electric field is the only pertrurbative parameter,

$$\begin{aligned}\bar{\mathcal{G}}(t,t_0;s) = \mathrm{Tr}\Bigg(& \exp \mathcal{L}_0(t-t_0) + \int_{t_0}^{t} \exp(\mathcal{L}_0 t)\tilde{\mathcal{L}}_{int}(t_1) \\ & \times \exp(-\mathcal{L}_0 t)dt_1 + \int_{t_0}^{t}\int_{t_0}^{t_2} \exp(\mathcal{L}_0 t)\tilde{\mathcal{L}}_{int}(t_2)\tilde{\mathcal{L}}_{int}(t_1) \\ & \times \exp(-\mathcal{L}_0 t)dt_2 dt_1 \\ & + \int_{t_0}^{t}\int_{t_0}^{t_3}\int_{t_0}^{t_2} \exp(\mathcal{L}_0 t)\tilde{\mathcal{L}}_{int}(t_3)\tilde{\mathcal{L}}_{int}(t_2)\tilde{\mathcal{L}}_{int}(t_1) \\ & \times \exp(-\mathcal{L}_0 t_0)dt_3 dt_2 dt_1 + \cdots \Bigg)\rho(t_0).\end{aligned} \tag{B6}$$

To simplify the result obtained by applying Eq. (B6) to our model Eq. (B1), we will assume that the initial state is diagonal in the system variables. We then get a simplified description using a two-dimensional subspace $(\rho_{ee}(\mathbf{q},\mathbf{q}');\rho_{gg}(\mathbf{q},\mathbf{q}'))$. To that end we introduce auxiliary 2×2 matrices $\mathcal{A}(t_1;t_0) \equiv \exp A(t_1 - t_0)$ and $C(t_2;t_1) \equiv \mathcal{V}(t_2)\exp[B(t_2-t_1)]\mathcal{V}(t_1)$ with elements

$$C(t_2;t_1) = E^2\begin{pmatrix} c_{ee}(t_2;t_1) & c_{eg}(t_2;t_1) \\ c_{ge}(t_2;t_1) & c_{gg}(t_2;t_1) \end{pmatrix},$$

$$\begin{aligned} c_{ee} = & -e^{(i\Delta-\Gamma/2)t_{21}} f^*(t_2)f(t_1)D_{ge}^{(R)}(t_2)D_{eg}^{(R)}(t_1) \\ & - e^{(-i\Delta-\Gamma/2)t_{21}} f(t_2)f^*(t_1)D_{eg}^{(L)}(t_2)D_{ge}^{(L)}(t_1), \end{aligned}$$

$$\begin{aligned} c_{eg} = & +e^{(i\Delta-\Gamma/2)t_{21}} f^*(t_2)f(t_1)D_{ge}^{(R)}(t_2)D_{eg}^{(L)}(t_1) \\ & + e^{(-i\Delta-\Gamma/2)t_{21}} f(t_2)f^*(t_1)D_{eg}^{(L)}(t_2)D_{ge}^{(R)}(t_1), \end{aligned}$$

$$\begin{aligned} c_{ge} = & +e^{(i\Delta-\Gamma/2)t_{21}} f^*(t_2)f(t_1)D_{ge}^{(L)}(t_2)D_{eg}^{(R)}(t_1) \\ & + e^{(-i\Delta-\Gamma/2)t_{21}} f(t_2)f^*(t_1)D_{eg}^{(R)}(t_2)D_{ge}^{(L)}(t_1), \end{aligned}$$

$$\begin{aligned} c_{gg} = & -e^{(i\Delta-\Gamma/2)t_{21}} f^*(t_2)f(t_1)D_{ge}^{(L)}(t_2)D_{eg}^{(L)}(t_1) \\ & - e^{(-i\Delta-\Gamma/2)t_{21}} f(t_2)f^*(t_1)D_{eg}^{(R)}(t_2)D_{ge}^{(R)}(t_1). \end{aligned} \tag{B7}$$

For brevity we adopt the following shorthand convention for time-ordered integrations.

$$\int_{t_0}^{t} dt_4 \cdots \int_{t_0}^{t_2} dt_1 \equiv \int_{t_0}^{t} dt_4 \int_{t_0}^{t_4} dt_3 \int_{t_0}^{t_3} dt_2 \int_{t_0}^{t_2} dt_1.$$

The generating function is calculated using Eqs. (B1), (B5), and (B6). Note that $\mathcal{W}A\mathcal{W}=0$ (the two level system cannot emit a second photon without an excitation in between), and omit terms independent of s which do not contibute to any factorial moment. To fourth order in the electric field we get

$$
\begin{aligned}
\mathcal{G}(t,t_0;s) = \mathrm{Tr}\Bigg[& \int_{t_0}^{t} \mathcal{A}(t;t_1)\mathcal{W}(t_1)\mathcal{A}(t_1;t_0) + \int_{t_0}^{t} dt_3 \int_{t_0}^{t_3} dt_2 \int_{t_0}^{t_2} dt_1 \mathcal{A}(t;t_3)\mathcal{W}(t_3)\mathcal{A}(t_3;t_2)C(t_2;t_1)\mathcal{A}(t_1;t_0) \\
& + \int_{t_0}^{t} dt_3 \int_{t_0}^{t_3} dt_2 \int_{t_0}^{t_2} dt_1 \mathcal{A}(t;t_3)C(t_3;t_2)\mathcal{A}(t_2;t_1)\mathcal{W}(t_1)\mathcal{A}(t_1;t_0) \\
& + \int_{t_0}^{t} dt_4 \cdots \int_{t_0}^{t_2} dt_1 \mathcal{A}(t;t_4)\mathcal{W}(t_4)\mathcal{A}(t_4;t_3)C(t_3;t_2)\mathcal{A}(t_2;t_1)\mathcal{W}(t_1)\mathcal{A}(t_1;t_0) \\
& + \int_{t_0}^{t} dt_5 \cdots \int_{t_0}^{t_2} dt_1 \mathcal{A}(t;t_5)\mathcal{W}(t_5)\mathcal{A}(t_5;t_4)C(t_4;t_3)\mathcal{A}(t_3;t_2)C(t_2;t_1)\mathcal{A}(t_1;t_0) \\
& + \int_{t_0}^{t} dt_5 \cdots \int_{t_0}^{t_2} dt_1 \mathcal{A}(t;t_5)C(t_5;t_4)\mathcal{A}(t_4;t_3)C(t_3;t_2)\mathcal{A}(t_2;t_1)\mathcal{W}(t_1)\mathcal{A}(t_1;t_0) \\
& + \int_{t_0}^{t} dt_5 \cdots \int_{t_0}^{t_2} dt_1 \mathcal{A}(t;t_5)C(t_5;t_4)\mathcal{A}(t_4;t_3)\mathcal{W}(t_3)\mathcal{A}(t_3;t_2)C(t_2;t_1)\mathcal{A}(t_1;t_0) \\
& + \int_{t_0}^{t} dt_6 \cdots \int_{t_0}^{t_2} dt_1 \mathcal{A}(t;t_6)C(t_6;t_5)\mathcal{A}(t_5;t_4)\mathcal{W}(t_4)\mathcal{A}(t_4;t_3)C(t_3;t_2)\mathcal{A}(t_2;t_1)\mathcal{W}(t_1)\mathcal{A}(t_1;t_0) \\
& + \int_{t_0}^{t} dt_6 \cdots \int_{t_0}^{t_2} dt_1 \mathcal{A}(t;t_6)\mathcal{W}(t_6)\mathcal{A}(t_6;t_5)C(t_5;t_4)\mathcal{A}(t_4;t_3)C(t_3;t_2)\mathcal{A}(t_2;t_1)\mathcal{W}(t_1)\mathcal{A}(t_1;t_0) \\
& + \int_{t_0}^{t} dt_6 \cdots \int_{t_0}^{t_2} dt_1 \mathcal{A}(t;t_6)\mathcal{W}(t_6)\mathcal{A}(t_6;t_5)C(t_5;t_4)\mathcal{A}(t_4;t_3)\mathcal{W}(t_3)\mathcal{A}(t_3;t_2)C(t_2;t_1)\mathcal{A}(t_1;t_0) \\
& + \int_{t_0}^{t} dt_7 \cdots \int_{t_0}^{t_2} dt_1 \mathcal{A}(t;t_7)\mathcal{W}(t_7)\mathcal{A}(t_7;t_6)C(t_6;t_5)\mathcal{A}(t_5;t_4)\mathcal{W}(t_4)\mathcal{A}(t_4;t_3)C(t_3;t_3)\mathcal{A}(t_2;t_1)\mathcal{W}(t_1)\mathcal{A}(t_1;t_0) \Bigg] \rho(t_0).
\end{aligned}
\tag{B8}
$$

The moments are obtained by differentiation with respect to s. The matrix element of W is denoted $w_{ge}(t) \equiv [\kappa(t;t_0;s)\Gamma/|\mu|^2] D_{ge}^{(L)}(t) D_{eg}^{(R)}(t)$. The average photon count is given to second order in the electric field:

$$
\begin{aligned}
\langle n \rangle(t;t_0) = & \int_{t_0}^{t} dt_1 e^{-\Gamma(t_1-t_0)} \mathrm{Tr}_B w_{ge}(t_1)\rho_{ee}(t_0) + E^2 \int_{t_0}^{t} dt_3 \int_{t_0}^{t_3} dt_2 \int_{t_0}^{t_2} dt_1 e^{-\Gamma(t_3-t_2)} \mathrm{Tr}_B w_{ge}(t_3) c_{eg}(t_2,t_1)\rho_{gg}(t_0) \\
& + E^2 \int_{t_0}^{t} dt_3 \int_{t_0}^{t_3} dt_2 \int_{t_0}^{t_2} dt_1 e^{-\Gamma(t-t_3)} e^{-\Gamma(t_1-t_0)} \mathrm{Tr}_B c_{eg}(t_3,t_2) w_{ge}(t_1)\rho_{ee}(t_0) \\
& + E^2 \int_{t_0}^{t} dt_3 \int_{t_0}^{t_3} dt_2 \int_{t_0}^{t_2} dt_1 e^{-\Gamma(t_1-t_0)} \mathrm{Tr}_B c_{gg}(t_3,t_2) w_{ge}(t_1)\rho_{ee}(t_0) \\
& + E^2 \int_{t_0}^{t} dt_1 \int_{t_0}^{t_3} dt_2 \int_{t_0}^{t_2} dt_1 e^{-\Gamma(t_3-t_2)} e^{-\Gamma(t_1-t_0)} \mathrm{Tr}_B w_{ge}(t_3) c_{ee}(t_2,t_1)\rho_{ee}(t_0) \\
& + 2\, E^2 \int_{t_0}^{t} dt_4 \cdots \int_{t_0}^{t_2} dt_1 e^{-\Gamma(t_4-t_3)} e^{-\Gamma(t_1-t_0)} \mathrm{Tr}_B w_{ge}(t_4) c_{eg}(t_3,t_2) w_{ge}(t_1)\rho_{ee}(t_0)
\end{aligned}
\tag{B9}
$$

and the second factorial moment to fourth order in the electric field is

$$
\begin{aligned}
\langle n(n-1) \rangle(t;t_0) = & 2E^2 \int_{t_0}^{t} \cdots \int_{t_0}^{t_2} e^{-\Gamma(t_4-t_3+t_1-t_0)} \mathrm{Tr}_B w_{ge}(t_4) c_{eg}(t_3,t_2) w_{ge}(t_1)\rho_{ee}(t_0) dt_1 \cdots dt_4 \\
& + 2E^4 \int_{t_0}^{t} dt_6 \int_{t_0}^{t_6} dt_5 \int_{t_0}^{t_5} dt_4 \int_{t_0}^{t_4} dt_3 \int_{t_0}^{t_3} dt_2 \int_{t_0}^{t_2} dt_1 \times [e^{-\Gamma(t_6-t_5)} e^{-\Gamma(t_3-t_2)} \mathrm{Tr}_B w_{ge}(t_6) c_{eg}(t_5,t_4) w_{ge}(t_3) c_{eg}(t_2,t_1)\rho_{gg}(t_0) \\
& + e^{-\Gamma(t_6-t_5)} e^{-\Gamma(t_3-t_2)} e^{-\Gamma(t_1-t_0)} \mathrm{Tr}_B w_{ge}(t_6) c_{eg}(t_5,t_4) w_{ge}(t_3) c_{ee}(t_2,t_1)\rho_{ee}(t_0) \\
& + e^{-\Gamma(t_6-t_5)} e^{-\Gamma(t_4-t_3)} e^{-\Gamma(t_1-t_0)} \mathrm{Tr}_B w_{ge}(t_6) c_{ee}(t_5,t_4) c_{eg}(t_3,t_2) w_{ge}(t_1)\rho_{ee}(t_0)
\end{aligned}
$$

$$+ e^{-\Gamma(t-t_6)}e^{-\Gamma(t_4-t_3)}e^{-\Gamma(t_1-t_0)}\mathrm{Tr}_B c_{eg}(t_6,t_5)w_{ge}(t_4)c_{eg}(t_3,t_2)w_{ge}(t_1)\rho_{ee}(t_0)]$$
$$+ 6E^4\int_{t_0}^{t}dt_7\cdots\int_{t_0}^{t_2}dt_1 e^{-\Gamma(t_7-t_6)}e^{-\Gamma(t_4-t_3)}e^{-\Gamma(t_1-t_0)}\mathrm{Tr}_B w_{ge}(t_7)c_{eg}(t_6,t_5)w_{ge}(t_4)c_{eg}(t_3,t_2)w_{ge}(t_1)\rho_{ee}(t_0). \quad \text{(B10)}$$

Higher-order contributions are calculated in Appendix C.

Some simplification is possible using

$$\mathrm{Tr}\, w_{ge}\rho = (\kappa\Gamma/|\mu|^2)\mathrm{Tr}\, D_{ge}(t)\rho D_{eg}(t)$$
$$= (\kappa\Gamma/|\mu|^2)\mathrm{Tr}\, D_{ge}^{\dagger}(t)D_{ge}(t)\rho = \kappa\Gamma. \quad \text{(B11)}$$

Below we consider a system which starts in $t=-\infty$ in the ground state $\rho(-\infty)=\rho_{eq}$. Using Eqs. (23), (25), and (B11) factorial moments Eqs. (B9) and (B10) simplify to

$$\langle n\rangle(t;t_0) = E^2\int_{t_0}^{t}dt_3\int_{-\infty}^{t_3}dt_2\int_{-\infty}^{t_2}dt_1 e^{-\Gamma(t_3-t_2)}\mathrm{Tr}_B c_{eg}(t_2,t_1)\rho_{eq} \quad \text{(B12)}$$

and

$$\langle n(n-1)\rangle(t;t_0)$$
$$= 2E^4\int_{t_0}^{t}dt_6\int_{t_0}^{t_6}dt_5\int_{t_0}^{t_5}dt_4\int_{t_0}^{t_4}dt_3\int_{-\infty}^{t_3}dt_2\int_{-\infty}^{t_2}dt_1$$
$$\times e^{-\Gamma(t_6-t_5)}e^{-\Gamma(t_3-t_2)}\mathrm{Tr}_B c_{eg}(t_5,t_4)w_{ge}(t_3)c_{eg}(t_2,t_1)\rho_{eq}. \quad \text{(B13)}$$

By expanding the matrix elements c_{eg} and w_{ge} in the dipole moments using Eq. (B7) we recast the factorial moments in terms of Liouville-space correlation functions Eq. (36). With this, Eqs. (B12) and (B13) lead to Eqs. (38) and (40). The leading term for the third factorial moment is given in Appendix D.

APPENDIX C: HIGHER-ORDER CONTRIBUTIONS TO FACTORIAL MOMENTS

In this appendix we present corrections to the leading terms [Eqs. (B9) and (B10)] for a system, initially on the electronic ground state. The average photon count to fourth order in the electric field,

$$\langle n\rangle(T;t_0) = E^2\varphi_2 + E^4\varphi_4 + \cdots, \quad \text{(C1)}$$

is given by five terms, represented by 20 Feynman diagrams,

$$\varphi_4 = \int_{t_0}^{t}dt_5\int_{t_0}^{t_5}dt_4\int_{t_0}^{t_4}dt_3\int_{t_0}^{t_3}dt_2\int_{t_0}^{t_2}dt_1$$
$$\times [e^{-\Gamma t_{54}}\mathrm{Tr}_B w_{ge}(t_5)c_{eg}(t_4,t_3)c_{gg}(t_2,t_1)\rho_{gg}(t_0)$$
$$+ e^{-\Gamma(t-t_5)}e^{-\Gamma(t_3-t_2)}\mathrm{Tr}_B c_{eg}(t_5,t_4)w_{ge}(t_3)c_{eg}(t_2,t_1)\rho_{gg}(t_0)$$
$$+ e^{-\Gamma t_{32}}\mathrm{Tr}_B c_{gg}(t_5,t_4)w_{ge}(t_3)c_{eg}(t_2,t_1)\rho_{gg}(t_0)$$
$$+ e^{-\Gamma t_{54}}e^{-\Gamma t_{32}}\mathrm{Tr}_B w_{ge}(t_5)c_{ee}(t_4,t_3)c_{eg}(t_2,t_1)\rho_{gg}(t_0)]$$
$$+ 2\int_{t_0}^{t}dt_6\cdots\int_{t_0}^{t_2}dt_1 e^{-\Gamma t_{65}}e^{-\Gamma t_{32}}\mathrm{Tr}_B w_{ge}(t_6)c_{eg}(t_5,t_4)$$
$$\times w_{ge}(t_3)c_{eg}(t_2,t_1)\rho_{gg}(t_0). \quad \text{(C2)}$$

The sixth-order contribution to the second factorial moment,

$$\langle n(n-1)\rangle(T;t_0) = E^4\phi_4 + 2E^6\phi_6 + \cdots, \quad \text{(C3)}$$

is given by six terms, represented by 48 Feynman diagrams,

$$\phi_6 = \int_{t_0}^{t}dt_8\int_{t_0}^{t}dt_8\int_{t_8}^{t}dt_7\int_{t_0}^{t_7}dt_6\int_{t_0}^{t_6}dt_5\int_{t_0}^{t_5}dt_4\int_{t_0}^{t_4}dt_3\int_{t_0}^{t_3}dt_2\int_{t_0}^{t_2}dt_1$$
$$\times [e^{-\Gamma t_{87}}e^{-\Gamma t_{54}}\mathrm{Tr}_B w_{ge}(t_8)c_{eg}(t_7,t_6)w_{ge}(t_5)c_{eg}(t_4,t_3)c_{gg}(t_2,t_1)\rho_{gg}(t_0)$$
$$+ e^{-\Gamma(t_{65}}e^{-\Gamma t_{32}}\mathrm{Tr}_B c_{gg}(t_8,t_7)w_{ge}(t_6)c_{eg}(t_5,t_4)w_{ge}(t_3)c_{eg}(t_2,t_1)\rho_{gg}(t_0)$$
$$+ e^{-\Gamma(t-t_8)}e^{-\Gamma t_{65}}e^{-\Gamma t_{32}}\mathrm{Tr}_B c_{eg}(t_8,t_7)w_{ge}(t_6)c_{eg}(t_5,t_4)w_{ge}(t_3)c_{eg}(t_2,t_1)\rho_{gg}(t_0)$$
$$+ e^{-\Gamma t_{87}}e^{-\Gamma t_{32}}\mathrm{Tr}_B w_{ge}(t_8)c_{eg}(t_7,t_6)c_{gg}(t_5,t_4)w_{ge}(t_3)c_{eg}(t_2,t_1)\rho_{gg}(t_0)$$
$$+ e^{-\Gamma t_{87}}e^{-\Gamma(t_{65}}e^{-\Gamma(t_{32}}\mathrm{Tr}_B w_{ge}(t_8)c_{ee}(t_7,t_6)c_{eg}(t_5,t_4)w_{ge}(t_3)c_{eg}(t_2,t_1)\rho_{gg}(t_0)]$$
$$+ 3\int_{t_0}^{t}dt_9\cdots\int_{t_0}^{t_2}dt_1 e^{-\Gamma t_{98}}e^{-\Gamma t_{65}}e^{-\Gamma t_{32}}\mathrm{Tr}_B w_{ge}(t_9)c_{eg}(t_8,t_7)w_{ge}(t_6)c_{eg}(t_5,t_4)w_{ge}(t_3)c_{eg}(t_2,t_1)\rho_{gg}(t_0). \quad \text{(C4)}$$

APPENDIX D: THE THIRD FACTORIAL MOMENT

The third factorial moment of photon counting statistics [Eq. (5)] is given by triple differentiation of generating function in s, Eq. (27). The leading term (sixth order in the electric field) for the steady state is

$$\langle n(n-1)(n-2)\rangle(t;t_0) = \frac{6E^6\Gamma^3}{|\mu|^4}\int_{t_0}^{t}\int_{t_0}^{t_9}\int_{t_0}^{t_8}\int_{t_0}^{t_7}\int_{t_0}^{t_6}\int_{t_0}^{t_5}\int_{t_0}^{t_4}\int_{-\infty}^{t_3}\int_{-\infty}^{t_2} dt_9\cdots dt_1[e^{-\Gamma(t_{98}+t_{65}+t_{32})}e^{(i\Delta-\Gamma/2)t_{87}}e^{(i\Delta-\Gamma/2)t_{54}}e^{(i\Delta-\Gamma/2)t_{21}}$$
$$\times\langle\langle D_{ge}^{(R)}(t_8)D_{eg}^{(L)}(t_7)D_{ge}^{(L)}(t_6)D_{eg}^{(R)}(t_6)D_{ge}^{(R)}(t_5)D_{eg}^{(L)}(t_4)D_{ge}^{(L)}(t_3)D_{eg}^{(R)}(t_3)D_{ge}^{(R)}(t_2)D_{eg}^{(L)}(t_1)\rangle\rangle_g$$
$$+ e^{-\Gamma(t_{98}+t_{65}+t_{32})}e^{(i\Delta-\Gamma/2)(t_{87}}e^{(-i\Delta-\Gamma/2)t_{54}}e^{(i\Delta-\Gamma/2)t_{21}}$$
$$\times\langle\langle D_{ge}^{(R)}(t_8)D_{eg}^{(L)}(t_7)D_{ge}^{(L)}(t_6)D_{eg}^{(R)}(t_6)D_{ge}^{(L)}(t_5)D_{ge}^{(R)}(t_4)D_{ge}^{(L)}(t_3)D_{eg}^{(R)}(t_3)D_{ge}^{(R)}(t_2)D_{eg}^{(L)}(t_1)\rangle\rangle_g$$
$$+ e^{-\Gamma(t_{98}+t_{65}+t_{32})}e^{(i\Delta-\Gamma/2)t_{87}}e^{(i\Delta-\Gamma/2)t_{54}}e^{(-i\Delta-\Gamma/2)t_{21}}$$
$$\times\langle\langle D_{ge}^{(R)}(t_8)D_{eg}^{(L)}(t_7)D_{ge}^{(L)}(t_6)D_{eg}^{(R)}(t_6)D_{ge}^{(R)}(t_5)D_{eg}^{(L)}(t_4)D_{ge}^{(L)}(t_3)D_{eg}^{(R)}(t_3)D_{eg}^{(L)}(t_2)D_{ge}^{(R)}(t_1)\rangle\rangle_g$$
$$+ e^{-\Gamma(t_{98}+t_{65}+t_{32})}e^{(i\Delta-\Gamma/2)t_{87}}e^{(-i\Delta-\Gamma/2)t_{54}}e^{(-i\Delta-\Gamma/2)t_{21}}$$
$$\times\langle\langle D_{ge}^{(R)}(t_8)D_{eg}^{(L)}(t_7)D_{ge}^{(L)}(t_6)D_{eg}^{(R)}(t_6)D_{eg}^{(L)}(t_5)D_{ge}^{(R)}(t_4)D_{ge}^{(L)}(t_3)D_{eg}^{(R)}(t_3)D_{eg}^{(L)}(t_2)D_{ge}^{(R)}(t_1)\rangle\rangle_g] + \text{c . c.} \quad \text{(D1)}$$

APPENDIX E: CORRELATION FUNCTIONS FOR THE BROWNIAN OSCILLATOR MODEL

In this appendix we present the sixth point bath correlation function. The dipole moment operator can be expressed using Eq. (43):

$$D_{ge}(t) = \mu\,\exp_+ - i\int_0^t U(t')dt'.$$

We assume that $\langle\hat{U}\rangle=0$, which can always be realized by a shift of ϵ and hold for Eq. (42) for symmetry reasons. Using the cumulant expansion [35] to the second order in U we get the two point bath correlation function,

$$J(t_1,t_2) = |\mu|^2\exp[-g(t_{12})]. \quad \text{(E1)}$$

Following Appendix 8A of Ref. [35] we obtain for the six point bath correlation function

$$F(t_1,t_2,t_3,t_4,t_5,t_6) = |\mu|^6\exp[-g(t_{12}) + g(t_{13}) - g(t_{14}) + g(t_{15}) - g(t_{16}) - g(t_{23}) + g(t_{24}) - g(t_{25}) + g(t_{26}) - g(t_{34}) + g(t_{35}) - g(t_{36}) - g(t_{45}) + g(t_{46}) - g(t_{56})], \quad \text{(E2)}$$

where $t_{ij}\equiv t_i - t_j$. For a harmonic bath Eqs. (E1) and (E2) are exact, since higher-order cumulants vanish. For the second factorial moment Eq. (41) we only need correlation function with $t_2=t_5$ and using $g(0)=0$; $g(t)=g^*(-t)$ we get Eq. (45).

[1] D. E. Kopppel, Phys. Rev. A **10**, 1938 (1974).
[2] S. B. Dubin and G. B. Benedek, Biophys. J. **9**, A212 (1969).
[3] H. Z. Cummins and H. L. Swinney, *Progress in Optics*, edited by E. Wolf (North-Holland, Amsterdam, 1970), Vol. VII.
[4] L. Mandel and E. Wolf, *Optical Coherence and Quantum Optics* (Cambridge University Press, New York, 1995).
[5] T. Basché, W. E. Moerner, M. Orrit, and H. Talon, Phys. Rev. Lett. **69**, 1516 (1992).
[6] S. Weiss, Science **283**, 1676 (1999).
[7] H. Bach, A. Renn, G. Zumofen, and U. P. Wild, Phys. Rev. Lett. **82**, 2195 (1999).
[8] H. Yang, G. Luo, P. Karnchanaphanurach, T-M. Louie, I. Rech, S. Cova, L. Xun, and X. S. Xie, Science **302**, 262 (2003).
[9] W. E. Moerner and L. Kador, Phys. Rev. Lett. **62**, 2535 (1989).
[10] M. Orrit and J. Bernard, Phys. Rev. Lett. **65**, 2716 (1990).
[11] F. Kulzer and M. Orrit, Annu. Rev. Phys. Chem. **55**, 585 (2004).
[12] E. Barkai, Y. Jung, and R. Silbey, Annu. Rev. Phys. Chem. **55**, 457 (2004).
[13] R. J. Glauber, Phys. Rev. **131**, 2766 (1963).
[14] P. L. Kelley and W. H. Kleiner, Phys. Rev. **136**, A316 (1964).
[15] H. J. Carmichael and D. F. Walls, J. Phys. B **9**, L43 (1976).
[16] H. J. Kimble, M. Dagenais, and L. Mandel, Phys. Rev. Lett. **39**, 691 (1977).
[17] L. Mandel, Opt. Lett. **4**, 205 (1979).
[18] S. C. Kou, X. S. Xie, and J. S. Liu, J. Royal Statistical Soc. C-Applied Statistics (to be published).
[19] J. Wang and P. Wolynes, Phys. Rev. Lett. **74**, 4317 (1995).
[20] V. Barsegov, V. Chernyak, and S. Mukamel, J. Chem. Phys. **116**, 4240 (2002).
[21] P. W. Anderson, B. I. Halperin, and C. M. Varma, Philos. Mag. **25**, 1 (1971).
[22] R. Kubo, J. Math. Phys. **4**, 174 (1963).
[23] Y. Jung, E. Barkai, and R. J. Silbey, Chem. Phys. **284**, 181 (2002).
[24] G. C. Hegerfeldt, Phys. Rev. A **47**, 449 (1993).
[25] M. B. Plenio and P. L. Knight, Rev. Mod. Phys. **70**, 101 (1998).
[26] D. E. Makarov and H. Metiu, J. Chem. Phys. **115**, 5989 (2001).
[27] N. G. van Kampen, *Stochastic Processes in Physics and Chemistry* (North-Holland, Amsterdam, 1992).
[28] Y. Zheng and F. L.H. Brown, Phys. Rev. Lett. **90**, 238305 (2003).
[29] Y. Zheng and F. L. H. Brown, J. Chem. Phys. **119**, 11814

(2003).
[30] Y. Zheng and F. L. H. Brown, J. Chem. Phys. **121**, 7914 (2004).
[31] E. Geva and J. L. Skinner, J. Phys. Chem. B **44**, 8920 (1997).
[32] F. L. H. Brown and R. J. Silbey, J. Chem. Phys. **108**, 7434 (1998).
[33] R. Blatt and P. Zoller, Eur. J. Phys. **9**, 250 (1988).
[34] M. Merz and A. Schenzle, Appl. Phys. B: Photophys. Laser Chem. **50**, 115 (1990).
[35] S. Mukamel, *Principles of Nonlinear Optical Spectroscopy* (Oxford University Press, New York, 1995).
[36] G. S. Agarwal, *Quantum Statistical Theories of Spontaneous Emission and their Relation to Other Approaches*, edited by G. Höhler, Springer Tracts in Modern Physics No. 70 (Springer, New York, 1974).
[37] S. Mukamel, Phys. Rev. A **68**, 063821 (2003).
[38] G. Herzberg, *Spectra of Diatomic Molecules* (Van Nostrand, New York, 1950).
[39] A. O. Caldeira and A. J. Leggett, Physica A **121**, 587 (1983).